Thrombospondin1 Enhanced Neuronal Wnt7a and CNTF Expressions by TNFα Signaling Pathway

xuebao wang
Wenzhou Medical University
He Yu
Wenzhou Medical University
Baihui Chen
Wenzhou Medical University
leping liu
Wenzhou Medical University
Shuya Feng
Wenzhou Medical University
saidan ding (firstdsdan@hotmail.com)
Wenzhou Medical University

Research

Keywords: cognitive impairment, synapse, Thrombospondin, TNFα, Wnt7a, CNTF

Posted Date: March 23rd, 2021

DOI: https://doi.org/10.21203/rs.3.rs-338128/v1

Abstract

Background: Thrombospondin (TSP) is an astrocyte-secreted protein, well-known for its function as a modulator of synaptogenesis and neurogenesis. The mechanism underlying the effects of TSP1 on synaptic activity and formation involved in MHE pathogenesis remains unclear.

Methods: The present study explored the effect of TSP1 on neurodegeneration, inflammatory response and the activation of Wnt7a/CNTF signaling in the primary rat neurons and an MHE rat model.

Results: When we treated neurons with TSP1, p38MAPK phosphorylation and TNFα expression was increased significantly. Also, the exposure of TSP1 increased the expression and release of Wnt7a and CNTF, upregulated spinophilin, enhanced the interaction of Wnt7a/CNTF with spinophilin, and triggered synaptic activity through p38/TNFα signaling in PC12 cells and primary neurons. The hippocampal injection of TSP1 siRNA in mice decreased the interaction of Wnt7a/CNTF with spinophilin, while injection of Wnt7a and CNTF improved learning and memory dysfunctions. MHE brains showed decreased TSP1 expression. The overexpression of TSP1 in the hippocampus of MHE rats ameliorated the disrupted synaptogenesis, learning, and memory.

Conclusions: Taken together, these results indicated that TSP1 is a potential synaptic factor related to the inflammatory response and the activation of Wnt7a/CNTF signaling in MHE pathogenesis.

Introduction

Minimal hepatic encephalopathy (MHE) represents a mild neurocognitive disorder in patients with liver cirrhosis and portosystemic shunts. These subtle neurocognitive abnormalities primarily affect attention, information processing, motor abilities, and coordination that are not recognizable on standard neurological examinations and independent of sleep dysfunction or problems with overall intelligence [1–4]. However, the specific molecular mechanism of MHE pathology is not yet understood.

Astrocyte-derived thrombospondins (TSPs) are large extracellular matrix proteins that have been identified as major contributors to astrocyte-regulated excitatory synapse formation [5]. The TSP family consists of two subfamilies, A and B, according to their organization and domain structure: A includes the trimeric TSP1 and TSP2, whereas B includes pentameric TSP3, TSP4, and TSP5 [6]. The expression of all TSPs has been detected in the brain, and studies using purified retinal ganglion cell cultures indicated that TSPs, especially TSP1 and TSP2, promote the formation of new excitatory (glutamatergic) synapses [7, 8]. Emerging evidence demonstrated that TSPs expressed by immature and reactive astrocytes are responsible for the excitatory central nervous system (CNS) synaptogenesis or synapse formation [9, 10]. Double TSP1 and TSP2 knockout mice show a reduced number of excitatory synapses in the cortex [7] and display dendritic spine irregularities [5]. Therefore, we focused our attention on the mechanisms underlying the involvement of TSP1 in the pathogenesis of MHE.

Overall, the expression of TSP1 and its effect on cognitive function is associated with Wnt7a/Ciliary Neurotrophic Factor(CNTF)/spinophilin interaction in MHE, which has not yet been investigated. The current study implied that increasing TSP1 levels in MHE would prevent the impairment of Wnt7a/CNTF with spinophilin interaction by inactivating p38/Tumor Necrosis Factor α (TNFα) signaling.

Materials And Methods

MHE models and treatment

A total of 40 Sprague-Dawley (SD) rats (Experimental Animal Center of the Chinese Academy of Sciences in Shanghai, China), weighing 220–250 g, were housed under controlled conditions of temperature (24 ± 1°C) and light (12 h light starting at 07:00 a.m.). All experiments were carried out in accordance with the guidelines laid down by the Ethics Committees of the Affiliated Hospital of Wenzhou Medical University regarding the care and use of animals for experimental procedures [11].

Before experiments, all animals underwent a series of behavioral tests: Y-maze (YM) and water-finding task (WFT). The normal values of these behavioral tests were obtained. Then, the rats were then randomly divided into two groups: control (n = 20) and thioacetamid (TAA) (n = 30). Liver cirrhosis was induced by intraperitoneal injection (i.p.) of TAA (200 mg/kg in normal saline, Sigma–Aldrich,Darmstadt, Germany) twice per week for 8 weeks. TAA-treated rats with symptoms were diagnosed as HE. The symptoms of HE were as follows: a subsequent decrease in motor activity, lethargy, and an eventual progression to coma. TAA-treated rats with no hepatic encephalopathy (HE) symptoms were again subjected to behavioral tests to confirm MHE. If TAA-treated rats met the criteria: a) values of YM were lower than mean ± 1.96 (SD); b) values of WFT were more than mean ± 1.96 (SD), the animals were included in the MHE group.

MHE rats were microinjected with TSP1 overexpression plasmid into hippocampus for 24 h.

YM test

Rats were individually placed at the end of an arm and allowed to explore the maze freely for 8 min. Total arm entries and spontaneous alternation percentage (SA%) were measured. SA% was defined as the ratio of the arm choices that differed from the previous two choices (“successful choices”) to total choices during the run (“total entry minus two” because the two entries could not be evaluated) [12].

WFT test

A rat was placed at the near-right corner of the apparatus and allowed to explore freely for 3 min. The rats that could not find the tube within 3 min were omitted from the analysis. After the training session, the animals were deprived of water for 24 h. In the trial session, they were again individually placed at the

same corner of the apparatus and allowed to find and drink the water in the alcove. The elapsed time until the entry into the alcove (entry latency, EL) until the touching/sniffing/licking of the water tube (contacting latency, CL) and until the initiation of drinking from the water tube (drinking latency, DL) was measured [13].

TSP1 knockdown mice

WT (wild-type) mice (Balb/c) were anesthetized with intramuscular xylazine (16 mg/kg), followed by ketamine (100 mg/kg). TSP1 small interfer ribonucleic acid (siRNA) was (10 or 40 μg/5μL) injected into the left hippocampus of mice for 24 h (anterior -posterior, + 0.3 mm; lateral, 1.0 mm; horizontal, 3.0 mm from the bregma) (n = 15).

Primary hippocampal neurons culture

Primary hippocampal rats neurons (PHNs) were prepared from 1-day-old SD rat pups and dissociated from freshly dissected hippocampus or cerebral cortex by mechanical disruption in the presence of trypsin and DNase and then plated in poly-L-lysine-precoated six-well plates. The cells were seeded at a density of 2×10^6 cells/well in Neurobasal® Medium (1X) supplemented with 0.5 mM GlutaMAX™-I and B-27® and incubated at 37°C, 5% CO_2 .

PC12 cell culture

The rat pheochromocytoma PC12 cell line was obtained from the American Type Culture Collection (ATCC, Manassas, VA, USA) and cultured in DMEM with 2 mM glutamine, 10% horse serum, and 5% heat-inactivated fetal bovine serum (FBS) that was passaged one time per week.

Cells treatment

The cells were stimulated with TSP1 (1, 5, or 20 μg/mL), human Wnt7a (100 ng/ml), human TNFα (20 ng/ml), Wnt inhibitor XAV939 (1 μmol/L), p38 mitogen-activated protein kinase (MAPK) inhibitor SB202190 (SB, 50 μmol/L), p38MAPK activator anisomycin (Ani, 10 μmol/L), and TNFα inhibitor lenalidomide (len, 50 μmol/L) for 3 h. Wells received 0.25 μg of p38/TNFα/Wnt7a/CNTF Lentiviral Activation Particles (Santa Cruz, CA, USA) along with 10 ng of the control plasmid pCMV-Tag2A for normalization of transfection efficiency.

Each well of cells received 0.25 μg of p38/TNFα/Wnt7a/CNTF siRNA (Santa Cruz, CA, USA) using Lipofectamine 2000 reagent (Invitrogen,Carlsbad, CA,USA), according to the manufacturer's protocol. An equivalent of 10 ng of The Silencer Negative Control number 1 siRNA (scrambled siRNA) was used as a control (Santa Cruz).

Real-time quantitative PCR (RT/q-PCR)

For RT-PCR, total RNA was isolated using the Qiagen RNA-Easy kit according to the manufacturer's protocol. Complementary deoxyribonucleic acid (cDNA) was synthesized using oligo (dT), deoxy-ribonucleoside triphosphate (dNTP), 0.1 M Dithiothreitol (DTT), Moloney murine leukemia virus reverse transcriptase, RNaseOUT (all from Invitrogen). The amplification was carried out using the PCR Master Mix (Promega,Wisconsin, USA). The amplified products were analyzed by electrophoresis on 2% agarose gels, visualized by EtBr staining, and quantitated against that of glyceraldehyde-3-phosphate dehydrogenase (GAPDH). qPCR was performed on the ABI-Prism7700 sequence detection system (Applied Biosystems Foster City, CA) using iTaq™ Fast Supermix with ROX (Bio-Rad Hercules, CA, USA) and 6-carboxyfluorescein-labeled TSP1, p38, TNFα, Wnt7a, CNTF, β-catenin, and GAPDH primers (Integrated DNA Technologies, Coralville, IA, USA). The mRNA expression was analyzed using the relative $2^{-\Delta\Delta CT}$ method. The following primers (Invitrogen) for murine genes:

TSP1, Forward: 5'- TTGCCAGCGTTGCCA-3',

Reverse: 5'- TCTGCAGCACCCCCTGAA-3';

P38, Forward: 5'-AGTGGCTGACCCTTATGAC-3',

Reverse: 5'-CACAGTGAAGTGGGATGGA-3';

TNFα, Forward: 5'-AGGTCTACTTTGGAGTCATTG – 3',

Reverse: 5'- TTCTGAGCAT-CGTAGTTGTTG – 3';

Wnt7a, Forward: 5'- CTGTGGCTGCGACAAAGAGAA-3',

Reverse: 5'- GCCGTGGCACTTACATTCC-3';

CNTF, Forward: 5'-AGGAAGATTCGTTCAGACCT-3',

Reverse: 5'-CCAGTGGCAAGCACTGATC-3';

GAPDH, Forward: 5'-TGTCATCAACGGGAAGCCCA-3',

Reverse: 5'-TTGTCATGGATGACCTTGGC-3'.

Measurement of TNFα/Wnt7a/CNTF release

Extracellular TNFα/Wnt7a/CNTF levels in the culture medium of primary neurons was measured using enzyme-linked immunosorbent assay (ELISA) kit (R&D Systems, Minneapolis, MN, USA) according to the manufacturer's instructions. Plates were analyzed spectrophotometrically on a Thermo-Fisher Multiskan MCC plate reader(Thermo Fisher Scientific, Waltham, MA).).

Immunoblotting (IB) analysis

The total amount of protein in the lysates was determined by the BCA protein assay (Amresco,USA). An equivalent of 50 μg protein was resolved by 10% sodium dodecyl sulfate polyacrylamide gelelectrophoresis (SDS-PAGE) and electroblotted to Polyvinylidene Fluoride (PVDF) membrane that was blocked with 5% non-fat dry milk in Tris buffer saline and Tween 20 (TBST) (150 mM NaCl, 50 mM Tris, 0.05% Tween 20). Subsequently, the membranes were probed with primary antibodies, TSP1, p38MAPK, TNFα, TNFR1, Wnt7a, frizzled2 (FZD2), CNTF, CNTFR, spinophilin, and β-actin (Abcam□Cambridge, MA, USA), followed by incubation with horseradish peroxidase-conjugated secondary antibody(Abcam, Cambridge, UK). After extensive washing, the immunoreactive bands were visualized by ECL reagent (Thermo□USA) after exposure on Kodak BioMax film (Kodak). The band intensities were quantified using QuantityOne software. The intensities were expressed as fold-change relative to the GAPDH levels.

For coimmunoprecipitation, the lysates of tissues were incubated with antibodies overnight (4°C) and subsequently with protein G-agarose beads (Millipore, USA) for 5 h (4°C). Followed by washes with lysis buffer, the eluent was separated by SDS-PAGE and electroblotted to PVDF membrane using primary and secondary antibodies.

Dendritic spine density analysis in primary neurons

For dendritic spine analysis, we used immunocytochemistry with anti-microtubule-associated protein 2 (anti-MAP2) and anti-vesicular glutamate transporter 1 antibodies. After fixation, the primary antibodies used were microtubule-associated protein 2B (MAP2B; 1:200; BD Transduction Laboratories, San Jose, CA, USA) and vesicular glutamate transporter 1 (vGlut1; 1:100; Neuromab, Davis, CA, USA). Primary antibodies were applied overnight at 4°C, followed by incubation with AlexaFluor-conjugated secondary antibody for 1 h (1:500; Life Technologies, Waltham, MA, USA) and glass cover slipping. A z stack of the optical sections was visualized on a confocal laser scanning microscope (FV10i-w; Olympus Corporation, Tokyo, Japan). At least 10 cultured neurons from two batches of cultures per group were used for quantitative analysis.

Functional labeling of presynaptic boutons with FM4-64

FM4-64 staining (Invitrogen) was performed according to the manufacturer's instructions. Briefly, primary neurons were incubated with 5 mg/mL FM4-64 (Invitrogen) and 50 mM KCl in Hank's balanced salt solution for 1 min at 4°C, and then washed with the solution to remove free FM4-64.

Double-labeled fluorescence staining

Frozen brain sections or neurons (4mm) cultured on glass coverslips were fixed with 4% paraformaldehyde for 30min and then treated with 0.1% Triton X-100 for 10 min at room temperature. Subsequently, the sections were blocked with 5% normal goat serum in phosphate-buffered saline (PBS) for 1 h at room temperature. Then, the sections were incubated overnight at 4°C with the following primary antibodies: TSP1, TNFR1, FZD2, CNTFR, spinophilin, and MAP2 (Abcam) that were detected by incubation for 30 min with fluoresceine isothiocyanate (FITC) (green)/Alexa Fluor 594 (red)-conjugated secondary antibody. The images were captured using a Leica TCS SP2 (Leica Microsystems, Heerbrugg, Switzerland) confocal laser scanning microscope. The imaging data were analyzed and quantified using Image Pro Plus software.

Electrophysiological Analysis

Rats were anesthetized with isoflurane, decapitated, and the hippocampi were cut into 400-mm thick transverse slices with a vibratome. After incubation at room temperature in a-CSF for 60–90 min, the slices were placed in a recording chamber on the stage of an upright microscope (Olympus CX-31) and perfused at a rate of 3 mL/min with a-CSF (containing 1 mM $MgCl_2$) at 23–24°C. A 0.1-MΩ tungsten monopolar electrode was used to stimulate the Schaffer collaterals. The field excitatory postsynaptic potentials (fEPSPs) were recorded in CA1 stratum radiatum by a glass microelectrode filled with a-CSF with resistance of 3–4 MΩ. Field potential input-output curves were constructed by measuring fEPSP slope responding to the stimulus intensity increased from 1 to 7 V, with a 0.5 V increment. The long-term potentiation (LTP) of fEPSPs was induced by three theta-burst stimulations (TBSs), i.e., four pulses at 100 Hz, repeated three times at a 200-ms interval. Paired-pulse facilitation (PPF) was examined by applying pairs of pulses, separated by 20–500-ms intervals. The magnitudes of LTP were expressed as the mean percentage of the baseline fEPSP initial slope.

Statistical analysis

Data are presented as mean ± SD. The statistical significance between-group comparisons was determined by one-way analysis of variance (ANOVA). $P < 0.05$ or $P < 0.01$ was considered to be statistically significant.

Results

TSP − 1 inactivated p38MAPK/TNFα signaling in vitro

TSP1 is responsible for CNS synaptic formation [7, 10]. The P38MAPK pathway activation results in impaired synaptic plasticity [14], and increased systemic TNF-α may have roles in hippocampal neurodegeneration [15]. Next, we measured whether TSP1 stimulated the inactivation of p38MAPK/TNFα signaling in neurons. IB analysis of cell lysates showed that TSP1 gradually decreased the phosphorylation of p38MAPK (Fig. 1A and B) and the expression of TNFα (Fig. 1C and D) in PC12 cells in

a dose-dependent manner. Similarly, TSP1 treatment significantly decreased the release of TNFα from PC12 cells compared to the unstimulated cells in a dose-dependent manner, as determined by ELISA (Fig. 1E). Moreover, the expression of TNFα in response to TSP1 was decreased in a time-dependent manner (Fig. 1F and G). In addition, TSP1 treatment significantly decreased the release of TNFα from PC12 cells in a time-dependent manner, as determined by ELISA (Fig. 1H). Simultaneously, TSP1 treatment decreased the expression of TNFα/TNFR1 that was blocked by p38MAPK activator anisomycin (Fig. 1I and J), as well as the release of TNFα from PHNs, which was diminished by anisomycin, as determined by ELISA (Fig. 1K). The cell-bound TNFα was further decreased in PHNs with TSP1 treatment, as determined by immunostaining, which was diminished by anisomycin (Fig. 1L). These data indicated that TSP1 treatment reduced TNFα production via dephosphorylation of p38 in neurons.

TSP1 activated Wnt7a signaling via p38/TNFα signaling

Wnt signaling also plays a relevant role in the presynaptic and postsynaptic structure [16]. Herein, we evaluated the effect of TSP1 on the activity of Wnt7a/β-catenin signaling in neurons. PC12 cells treated with TSP1 did not show any change in the Wnt3a and Wnt5a levels, but a significant increase was noted in the expression of Wnt7a in a dose-dependent manner, as assessed by immunoblotting (Fig. 2A and B). Similarly, TSP1 treatment significantly increased the release of Wnt7a from PC12 cells compared to the unstimulated cells in a dose-dependent manner, as determined by ELISA (Fig. 2C). Also, PC12 cells exposed to TSP1 showed a significant increase in the expression of Wnt7a in a time-dependent manner by immunoblotting analysis (Fig. 2D and E) and ELISA (Fig. 2F). Simultaneously, PHNs were transfected with p38 (Fig. 2G) or TNFα (Fig. 2H) siRNA plasmids, and the results of transfection efficiency assessed by qPCR showed the p38 or TNFα mRNA level was significantly decreased, while the content of Wnt7a was increased in response to TSP1 post-transfection of PC12 cells with p38 or TNFα siRNA (Fig. 2I and J). Simultaneously, PHNs were transfected with p38 (Fig. 2K) or TNFα (Fig. 2L) overexpression plasmid, and the results of transfection efficiency showed p38 or TNFα mRNA level was significantly increased by qPCR. Immunoblotting analysis showed that TSP1 treatment significantly increased the expression of FZD2 in PC12 cells, which was diminished by p38 or TNFα overexpression (Fig. 2M and N). Also, Wnt7a was released from PHNs after TSP1 treatment, which was inhibited by anisomycin, as determined by ELISA (Fig. 2O). Moreover, Wnt7a expression was markedly increased by TSP1 treatment, as assessed by immunoblotting, which could be blocked by p38 activator anisomycin and TNFα (Fig. 2P and Q), and SB202190 or TNFα inhibitor, lenalidomide, enhanced the ability of TSP1 to stimulate the protein expression in PHNs (Fig. 2R and S). An increase in cell-bound pGSK3β was observed in PHNs after TSP1 treatment; this phenomenon was reversed by the addition of TNFα, as determined by immunostaining (Fig. 2T). Together, these data indicated that TSP1 treatment induced Wnt7a production via dephosphorylation of p38 and downregulation of TNFα in neurons.

TSP1 activated CNTF signaling via p38/TNFα

CNTF exerts neuroprotective effects[17–19]. Next, we determined the effect of TSP1 on the activity of CNTF signaling associated with Wnt7a signaling in primary neurons. The immunoblotting of PC12 cell lysates showed a maximal increase in the expression of CNTF and CNTFR by middle dose of TSP1 in (Fig. 3A and B). The TSP1 treatment significantly increased the release of CNTF from PC12 cells in a dose-dependent manner, as determined by ELISA (Fig. 3C). The cells exposed to TSP1 exhibited a significant increase in the expression of CNTF in a time-dependent manner by immunoblotting analysis (Fig. 3D and E). Similarly, TSP1 treatment significantly increased the release of CNTF from PC12 cells compared to unstimulated cells in a time-dependent manner, as determined by ELISA (Fig. 3F). An increase in the content of CNTF in response to TSP1 was amplified by p38 or TNFα siRNA in PC12 cells (Fig. 3G and H). Immunoblotting analysis showed that TSP1 treatment significantly increased the expression of CNTFR in PC12 cells, which was diminished by p38 or TNFα overexpression (Fig. 3I and J). TSP1treatment significantly increased CNTF expression, which was blocked by p38 activator anisomycin or Wnt inhibitor XAV939 (Fig. 3K and L); CNTFR expression was also markedly increased by TSP1 treatment, SB202190, lenalidomide, or Wnt7a; these molecules enhanced the ability of TSP1 to stimulate the protein expression (Fig. 3M and N) in PHNs. An increase in cell-bound CNTFR was observed in PHNs after TSP1 treatment; the addition of XAV939 reversed the effect, as determined by immunostaining (Fig. 3O). These data indicated that TSP1 treatment induced CNTF production through the inactivation of p38/TNFα signaling and activation of Wnt7a signaling in neurons.

TSP1 increased the interaction of Wnt7a/CNTF /spinophilin and synaptic activity via p38/TNFα signaling in vitro

Spinophilin is related to neuronal plasticity, which plays a role in learning.[20–22], [23]. Herein, we investigated whether TSP1 could stimulate the interaction among Wnt7a/CNTF with spinophilin. Immunoblotting from cell lysates showed that a maximal increase in the expression of spinophilin was achieved by the middle dose of TSP1 in PC12 cells (Fig. 4A and B). Time course analyses of PC12 cells treated with TSP1 showed a steady increase in spinophilin expression up to 48 h via immunoblotting (Fig. 4C and D).

Simultaneously, PHNs were transfected with Wnt7a (Fig. 4E) or CNTF (Fig. 4F) siRNA plasmids, and the results of transfection efficiency showed Wnt7a or CNTF mRNA level was significantly decreased by qPCR. Immunoblotting analysis showed that an increase in the content of spinophilin in response to TSP1 was abated by Wnt7a or CNTF siRNA in PC12 cells (Fig. 4G and H). Simultaneously, PHNs were transfected with Wnt7a (Fig. 4I) or CNTF (Fig. 4J) overexpression plasmids, and the results of transfection efficiency showed that Wnt7a or CNTF mRNA level was significantly decreased by qPCR. Wnt7a or CNTF overexpression enhanced the ability of TSP1 to stimulate spinophilin expression (Fig. 4K and L).

Next, we examined the effect of TSP1 on Wnt7a/CNTF with spinophilin interaction in neurons using coimmunoprecipitation. As shown in Fig. 4M, Wnt7a was immunoprecipitated, TSP1 treatment increased

the content of CNTF, and spinophilin coimmunoprecipitated with Wnt7a in PHNs, which was enhanced by SB202190 or lenalidomide. CNTF was also immunoprecipitated, and TSP1 elevated the level ofWnt7a, while spinophilin was coimmunoprecipitated with CNTF, which was further amplified by SB202190 or lenalidomide. TSP1 increased the level of Wnt7a and CNTF coimmunoprecipitated with spinophilin, which was further amplified by SB202190 or lenalidomide.

Using FM4-64 dye for probing activity-dependent synaptic vesicle recycle, TSP1 treatment markedly increased the synaptic activity, which was blocked by the addition of TNFα (Fig. 4N and O). Double immunofluorescence (IF) staining with anti-vGluT1 (for staining dendritic spines) with anti-MAP2 (for staining microtubules) antibodies, and TSP1 treatment significantly increased vGluT1-positive signals in PHNs, which was remarkably diminished by the addition of XAV939 (Fig. 4P and Q). These data indicated that TSP1 treatment induced spinophilin expression via interaction with Wnt7a/CNTF and inactivation of p38/TNFα signaling in neurons.

TSP1 knockdown decreased spinophilin expression and synaptic activity via Wnt7a/CNTF signaling in vivo

TSP1 knockdown impaired Wnt7a/CNTF with spinophilin interaction associated with cognitive loss in vivo. Then, we examined the association of cognitive function/LTP with Wnt/CNTF in TSP1 knockdown mice. First, TSP1 siRNA plasmid was injected into the hippocampus of mice, and the results of transfection efficiency showed that the TSP1 mRNA level in the hippocampus was significantly decreased, as assessed by qPCR (Fig. 5A). In YM, a significant reduction in SA% was found in the hippocampus of mice after TSP1 siRNA injection but was restored to the normal level by the administration of Wnt7a or CNTF (Fig. 5B). In WFT, TSP1 knockdown markedly increased the level of EL, CL, and DL in mice, which was reversed by Wnt7a or CNTF (Fig. 5C). Then, we tested LTP and the basal synaptic transmission at CA1 synapses by measuring the input/output (I/O) curves. As shown in Fig. 5D and E, TSP1 knockdown in mice significantly decreased the LTP magnitude and impaired the basal synaptic transmission, and administration of Wnt7a or CNTF rescued this LTP deficit and the impairment of basal synaptic transmission. Also, the interaction of Wnt7a/CNTF with spinophilin was examined in TSP1 knockdown mice. As shown in Fig. 5F, Wnt7a was immunoprecipitated, and TSP1 knockdown decreased the content of CNTF and spinophilin coimmunoprecipitated with Wnt7a in the hippocampus of mice, which was diminished by lenalidomide. Moreover, CNTF was immunoprecipitated, and TSP1 knockdown induced a significant decrease in Wnt7a and spinophilin coimmunoprecipitated with CNTF, which was further blocked by lenalidomide. In addition, TSP1 knockdown decreased the level of Wnt7a and CNTF coimmunoprecipitated with spinophilin, which was abated by lenalidomide. A decrease in cell-bound spinophilin was observed in the hippocampus of mice after TSP1 knockdown, and the administration of Wnt7a or CNTF reversed the level of this protein, as determined by immunostaining (Fig. 5G). These data indicated that the disruption of Wnt7a/CNTF and spinophilin interaction impaired the cognitive function and LTP in TSP1 knockdown mice.

TSP1 was downregulated in MHE rats

Next, we examined the expression of TSP-1 in MHE brains. As shown in Fig. 6A and B, decreased TSP1 level was observed in the hippocampus of MHE rats by IB analysis similar to that in the cortexes of MHE rats. The qPCR showed that TSP1 mRNA transcription was weak in the hippocampus and cortexes of MHE rats (Fig. 6C). IF staining revealed that pronounced that astrocytic TSP1 level was significantly decreased in the cortex of MHE rats compared to the controls (Fig. 6D). These observations indicated a decreased expression of TSP1 in the MHE brain.

TSP1 overexpression alleviated the impaired Wnt7a/CNTF and spinophilin interaction in the cognitive decline in MHE rats. We also tested the effect of TSP1 overexpression on the cognitive deficit in MHE rats. Flag-TSP1 overexpression plasmid was used for injection into the hippocampus of MHE rats. The results of transfection efficiency showed the TSP1 mRNA level in the hippocampus was significantly increased by qPCR compared to that in MHE rats (Fig. 7A). In YM, a significant reduction was detected in SA% in MHE rats, which was recovered to the normal level by TSP1 overexpression (Fig. 7B). In WFT, MHE rats showed a marked increase in EL, CL, and DL, and the significant delay in EL, CL, and DL was reversed by TSP1 overexpression in the hippocampus (Fig. 7C).

Furthermore, we tested the LTP and the basal synaptic transmission at CA1 synapses by measuring the I/O curves. As shown in Fig. 7D and E, TSP1 knockdown in MHE rats showed decreased LTP magnitude and impaired basal synaptic transmission, and overexpression of TSP1 rescued this LTP deficit and the impairment of the basal synaptic transmission.

Therefore, we explored whether TSP1 overexpression is involved in Wnt7a/CNTF and spinophilin interaction in MHE brains. As determined by immunostaining, a decrease in cell-bound spinophilin (Fig. 7F) was observed in the hippocampus of MHE rats, and TSP1 overexpression reversed the level of this protein. The effect of TSP1 overexpression on Wnt7a/CNTF and spinophilin interaction was evaluated using coimmunoprecipitation. As shown in Fig. 7G, Wnt7a was immunoprecipitated, and the hippocampus of MHE rats showed a decreased content of CNTF, and spinophilin coimmunoprecipitated with Wnt7a was diminished by TSP1 overexpression. CNTF was also immunoprecipitated, and the hippocampus of MHE rats displayed a significant decrease in Wnt7a, and spinophilin coimmunoprecipitated with CNTF was further blocked by TSP1 overexpression. Spinophilin was also immunoprecipitated, and the hippocampus of MHE rats displayed the obvious decrease in Wnt7a, and CNTF coimmunoprecipitated with spinophilin, which was further abated by TSP1 overexpression.

These data indicated that TSP1 overexpression rescues cognitive function and LTP associated with Wnt7a/CNTF and spinophilin interaction in the MHE brain.

Discussion

In the present study, we demonstrated that TSP1 expression was decreased in the brain of MHE rats. The injection of Flag overexpression plasmid into the hippocampus of MHE rats improves their learning and

memory. Our results suggested that the disturbance of hippocampal and cortical TSP1 generation might be involved in the deficit in learning and memory under the interaction of Wnt7a/CNTF with spinophilin.

Recent evidence suggested that astrocytes regulate synapse formation and integrity through the secretion of the extracellular matrix proteins TSPs, especially TSP1 [7, 24]. TSPs, critical astrocyte-secreted proteins, are large oligomeric extracellular matrix proteins that have been previously shown to play major roles in excitatory CNS synaptogenesis or synapse formation [9, 10]. TSP1, a member of a family of astrocyte-secreted extracellular matrix proteins, participates in synaptogenesis [5, 7].

Notably, our data presented that shortage of astroglia-derived TSP1 contributes to synaptic dysfunction in MHE rats and TSP1 knockdown mice, suggesting that decreased level of TSP1 is a common feature of MHE disease. Considering the involvement of TSP1 in cognitive and memory disorder, the current data suggested that TSP1 release in the hippocampus of rats play a major role in impaired learning and memory in MHE rats. Reportedly, TSP1 serves as a protective signaling molecule by preventing synaptic loss and acts as a neuro-modulator by facilitating the formation of hippocampal long-term potentiation (LTP) and the major cellular mechanisms underlying learning and memory. Another potential mechanism is the reduction in TSP1 levels, which might impact neuronal integrity with respect to the pathogenesis of MHE.

The MAPK family, including extracellular signal-regulated kinase (ERK), p38, and jun N-terminal kinase (JNK), mediates inflammation, cell proliferation, and apoptosis [25]. p38MAPK is a member of the MAPK family, which also includes extracellular signal-regulated kinase, big MAP kinase1, and c-Jun NH2-terminal kinase [26]. P38 MAPK pathway contributes to cognitive damage in pentylenetetrazole (PTZ)-induced epilepsy.[27] Inhibiting the p38 pathway alleviated $A\beta_{1-42}$-induced cognitive deficits and neuronal loss and death[28], while activation of p38-MAPK signaling pathway contributes to the formation disorder of cortical synapses [[29]]. A local increase in TNFα in the hippocampal dentate gyrus activates TNF receptor type 1 (TNFR1), which in turn, results in persistent functional impairment of hippocampal excitatory synapses [30]. Moreover, TNF-α confers susceptibility to schizophrenia and cognitive dysfunction [31], mediates cognitive deficits [32], and the synaptic action interferes with brain circuits pertaining to learning and cognition, which contributes to excitotoxicity and neurodegeneration [33]. Furthermore, TNF is a proteolytically cleaved transmembrane protein that exerts its activity via TNFR1 [34]. This cytokine is a major regulator of synapse function implicated in synaptic transmission and homeostatic synaptic scaling [35, 36]. Neurons in individuals are hypersensitive to TSP1 and exhibit pronounced dysregulation in the levels of p38MAPK/TNFα. Thus, upregulated TSP1 in neurons might downregulate neuronal p38MAPK/TNFα protein levels. Moreover, the increase in the p38MAPK/TNFα content in neurons was induced by transfection with TSP1 siRNA, while reduced TSP1 levels in astrocytes may stimulate both p38MAPK/TNFα signaling pathway in neurons.

Recent studies have proposed a critical role for Wnt pathway in the adult hippocampus involved in neurogenesis and synaptic plasticity [37–39], indicating a role of Wnt signaling also in maintaining the network connectivity, memory formation, and cognitive flexibility [40–43]. Canonical Wnt/b-catenin

signaling is altered or involved in the regulation of adult hippocampal neurogenesis and self-renewal of neural stem/progenitor cells [44, 45], the pathophysiology of Alzheimer's disease (AD), and other neurodegenerative disorders [46]. Specifically, postmortem studies have described reduced levels and altered activity of the intracellular component b-catenin in AD brains [47, 48]. Thus, aberrant Wnt signaling has been a proposed mechanism underlying the onset and progression of the pathological hallmarks in MHE [49].

Wnt ligands have been linked to the assembly of structural components in presynaptic compartments. Wnt7a induces axonal spreading and incremental growth of cone size and branching, leading to the accumulation of synaptic proteins [50, 51]. Then, in the cerebellum, Wnt7a acts as a retrograde signal from granular cells to induce presynaptic differentiation in mossy fibers, serving as a synaptogenic factor [51, 52]. Wnt7a also increases the clustering of postsynaptic proteins, such as postsynaptic density protein-95 [37]. Additionally, the use of FM dyes showed that TSP-1 stimulates recycling and accelerates exocytosis of synaptic vesicles. Wnt7a increases the amplitude of field excitatory postsynaptic potentials (fEPSP) and decreases the rate of paired-pulse facilitation in the CA3–CA1 synapse [37]. TSP1 rapidly activates Wnt in primary neurons, decreasing the p38/TNFα content by transfection with overexpression or siRNA plasmid or by stimulation of synthesis with inhibitors or activators. These processes prevent the deleterious effects of downregulated TSP1 on Wnt7a signaling. These findings implicated the TNFα/Wnt7a signaling cascade in the synaptic effects of TSP1. Therefore, we proposed that the p38/TNFα signaling is involved in decreased TSP1-induced hippocampal inactivation of Wnt signaling in MHE rats.

CNTF belongs to the IL-6 family of cytokines and exerts neuroprotective effects, thereby serving as a survival factor for sympathetic, sensory, hippocampal, and motor neurons in vitro as well as in vivo. Exogenous CNTF protects mature neurons from degeneration arising from multiple etiologies, including Huntington's disease, amyotrophic lateral sclerosis, or retinal degeneration, and its efficacy is tested in several clinical trials[17–19]. CNTF led to full recovery of cognitive functions associated with the stabilization of synaptic protein levels in the Tg2576 AD mice model. In vitro as well as in vivo, CNTF prevented synaptic and neuronal degeneration. These preclinical studies suggested that CNTF and/or CNTF receptor-associated pathways might exhibit AD-modifying activity through protection against progressive Aβ-related memory deficits. [53] CNTF enhances nicotinic synaptic transmission via both presynaptic and postsynaptic mechanisms[54]. TSP1 abolishes the effects of p38/TNFα on CNTF signaling, decreasing the p38/TNFα content in neurons by transfection with overexpression or siRNA plasmid or by stimulation of its synthesis with inhibitors or activators, thereby preventing the deleterious effects of the downregulation of TSP1 on CNTF signaling. Next, TSP1 increased the neuronal content of Wnt7a protein critically involved in the activation of CNTF signaling. These findings implicated the TNFα/Wnt7a/CNTF signaling cascade in the synaptic effects of TSP1. Therefore, we proposed that the disruption in Wnt signaling is involved in decreased TSP1-induced hippocampal inactivation of CNTF signaling in MHE rats.

Spinophilin expression was low during mice development but increased markedly after birth and persisted in the adult brain[55]. The immunolabeling approach revealed that spinophilin was found predominantly in dendritic spines in adult macaque prefrontal cortex[56]. Further studies showed that the protein is enriched in the cerebral cortex, caudatoputamen, hippocampal formation, and cerebellum[57], as well as at the synapse and in cadherin-based cell-cell adhesion sites[58]. Spinophilin is an optimal candidate to serve as a link between excitatory synapse transmission and changes in spine morphology and density. In initial experiments, spinophilin was implicated in the stabilization of the actin cytoskeleton in dendritic spines and in filipodia[59, 60]. It also regulates excitatory synaptic transmission and plasticity[57]. Furthermore, spinophilin is a postsynaptic marker, primarily localized in the heads of dendritic spines. The decrease in spinophilin immunoreactivity was significantly related to both Braak neurofibrillary tangle (NFT) staging and clinical severity but not Abeta deposition staging [61] It also has a critical role in learning in vivo and could be related to neuronal plasticity and learning [20–22]. Dysregulated spinophilin function might be implicated in synaptic failure and cognitive dysfunction linked to MHE. This evidence supported that TSP1 induced synaptic activity that was directly associated with spinophilin levels; our findings implicated the interaction of Wnt7a/CNTF with spinophilin in the synaptic effects of TSP1. In the brain, TSP1 promotes structural and functional recovery of synapses compromised by MHE via the mechanism involving the interaction of Wnt7a/CNTF with spinophilin. Therefore, enhanced interaction among Wnt7a/CNTF and spinophilin mediated by TSP1 has been shown to confer neuroprotection against synaptic impairment of MHE.

Conclusion

The current data provided comprehensive evidence of TSP1 involvement in the generation of Wnt7a/CNTF and the interaction of Wnt7a/CNTF with spinophilin via p38/TNFα signaling and synaptic plasticity. The present study demonstrated that the disturbance of endogenous TSP1 generation is involved in the loss of activation of Wnt/CNTF signaling in the hippocampus, which leads to a deficit in learning and memory. Therefore, preventing TSP1 might be a novel therapeutic strategy for MHE.

Abbreviations

MAP2: microtubule-associated protein 2; ATCC: American Type Culture Collection; BSA: Albumin from bovine serum; cDNA: complementary deoxyribonucleic acid; CNS: central nervous system; CNTF: Ciliary Neurotrophic Factor; DNAse: deoxyribonuclease; dNTP: deoxy-ribonucleoside triphosphate; DTT: Dithiothreitol; EDTA: Ethylene Diamine Tetraacetic Acid; ELISA: Enzyme-linked immunosorbent assay; ERK: extracellular signal-regulated kinase; FBS: fetal bovine serum; fEPSPs: field excitatory postsynaptic potentials; FITC: fluoresceine isothiocyanate; GAPDH: glyceraldehyde-3-phosphate dehydrogenase; HE: hepatic encephalopathy; IP: intraperitoneal injection; JNK: jun N-terminal kinase; LTP:long-term potentiation; MAP2B: microtubule-associated protein 2B; MAPK: mitogen-activated protein kinase; MHE: minimal hepatic encephalopathy; NFT: neurofibrillary tangle; PBS: phosphate buffer saline; PHNs: primary hippocampal rats neurons; PPF: paired-pulse facilitation; PTZ: pentylenetetrazole; PVDF:

Polyvinylidene Fluoride; qPCR: Real-time quantitative PCR; SD: Sprague–Dawley; SDS-PAGE: sodium dodecyl sulfate polyacrylamide gelelectrophoresis; SiRNA: small interfering ribonucleic acid; TAA: thioacetamide; TBSs: theta-burst stimulations; TNFα: Tumor Necrosis Factor α; TNFR1: TNF receptor type 1; TSP: thrombospondin; TSPs: thrombospondins; WFT: water-finding task; WT: wild-type; YM: Y-maze.

Declarations

Ethics approval and consent to participate

The study was approved by the Ethics Committee of the First Affiliated Hospital of Wenzhou Medical University.

Consent for publication

Not applicable

Data availability statement

The data that support the findings of this study are available from the corresponding author upon reasonable request.

Competing interests

The authors have declared no conflict of interest.

Funding

This study was supported by Basic Scientific Research Projects of Wenzhou city (Y20180076)Natural Science Foundation of Zhejiang province (LY21H030012) and Natural Science Foundation of China (81671042, 81300308).

Authors‘ Contributions

Saidan Ding supervised the entire project, designed the research and analysed the data and critically revised the manuscript. Shuya Feng and Baihui Chen conceived and designed the experiments, performed the research interpreted, and analysed the data, and wrote the paper. Xuebao Wang conceived and designed the experiments, interpreted and analysed the data, and supervised all the experimental procedure. Leping Liu and He Yu performed the research and analysed the data. All authors read and approved the final manuscript.

Acknowledgments

We thank Dr. Haoqi Ni for optimizing the image analysis method. We thank Dr. Yangping Shentu for technical supports. We thank Dr. Yunchang Mo for critical reading of the manuscript.

References

1. Ferenci P, Lockwood A, Mullen K, Tarter R, Weissenborn K, Blei AT: Hepatic encephalopathy--definition, nomenclature, diagnosis, and quantification: final report of the working party at the 11th World Congresses of Gastroenterology, Vienna, 1998. Hepatology 2002, 35(3):716-721.
2. Mullen KD: Review of the final report of the 1998 Working Party on definition, nomenclature and diagnosis of hepatic encephalopathy. Alimentary pharmacology & therapeutics 2007, 25 Suppl 1:11-16.
3. Kharbanda PS, Saraswat VA, Dhiman RK: Minimal hepatic encephalopathy: diagnosis by neuropsychological and neurophysiologic methods. Indian journal of gastroenterology : official journal of the Indian Society of Gastroenterology 2003, 22 Suppl 2:S37-41.
4. Ortiz M, Jacas C, Cordoba J: Minimal hepatic encephalopathy: diagnosis, clinical significance and recommendations. J Hepatol 2005, 42 Suppl(1):S45-53.
5. Garcia O, Torres M, Helguera P, Coskun P, Busciglio J: A Role for Thrombospondin-1 Deficits in Astrocyte-Mediated Spine and Synaptic Pathology in Down's Syndrome. Plos One 2010, 5(12):e14200.
6. Lawler J: Thrombospondin-1 as an endogenous inhibitor of angiogenesis and tumor growth. Journal of Cellular & Molecular Medicine 2002, 6(1):1.
7. Christopherson KS, Ullian EM, Stokes CCA, Mullowney CE, Hell JW, Agah A, Lawler J, Mosher DF, Bornstein P, Barres BA: Thrombospondins are astrocyte-secreted proteins that promote CNS synaptogenesis. Cell 2005, 120(3):421-433.
8. Crawford DC, Jiang X, Taylor A, Mennerick S: Astrocyte-derived thrombospondins mediate the development of hippocampal presynaptic plasticity in vitro. Journal of Neuroscience the Official Journal of the Society for Neuroscience 2012, 32(38):13100-13110.
9. Christopherson KS, Ullian EM, Stokes CC, Mullowney CE, Hell JW, Agah A, Lawler J, Mosher DF, Bornstein P, Barres BA: Thrombospondins are astrocyte-secreted proteins that promote CNS synaptogenesis. Cell 2005, 120(3):421-433.
10. Chen H, Herndon M, Lawler J: The cell biology of thrombospondin-1. Matrix Biology Journal of the International Society for Matrix Biology 2001, 19(7):597-614.
11. Albrecht J, Hilgier W, Zielinska M, Januszewski S, Hesselink M, Quack G: Extracellular concentrations of taurine, glutamate, and aspartate in the cerebral cortex of rats at the asymptomatic stage of thioacetamide-induced hepatic failure: modulation by ketamine anesthesia. Neurochemical research 2000, 25(11):1497-1502.

12. Yamada M, Chiba T, Sasabe J, Nawa M, Tajima H, Niikura T, Terashita K, Aiso S, Kita Y, Matsuoka M et al: Implanted cannula-mediated repetitive administration of Abeta25-35 into the mouse cerebral ventricle effectively impairs spatial working memory. Behav Brain Res 2005, 164(2):139-146.
13. Kawasumi M, Chiba T, Yamada M, Miyamae-Kaneko M, Matsuoka M, Nakahara J, Tomita T, Iwatsubo T, Kato S, Aiso S et al: Targeted introduction of V642I mutation in amyloid precursor protein gene causes functional abnormality resembling early stage of Alzheimer's disease in aged mice. Eur J Neurosci 2004, 19(10):2826-2838.
14. Ye Q, Zeng C, Luo C, Wu Y: Ferrostatin-1 mitigates cognitive impairment of epileptic rats by inhibiting P38 MAPK activation. Epilepsy Behav 2020, 103(Pt A):106670.
15. Hennessy E, Gormley S, Lopez-Rodriguez AB, Murray C, Murray C, Cunningham C: Systemic TNF-α produces acute cognitive dysfunction and exaggerated sickness behavior when superimposed upon progressive neurodegeneration. Brain Behav Immun 2017, 59:233-244.
16. Ciani L, Boyle KA, Dickins E, Sahores M, Anane D, Lopes DM, Gibb AJ, Salinas PC: Wnt7a signaling promotes dendritic spine growth and synaptic strength through Ca2+/Calmodulin-dependent protein kinase II. Proceedings of the National Academy of Sciences of the United States of America 2011, 108(26):10732-10737.
17. Bongioanni P, Reali C, Sogos V: Ciliary neurotrophic factor (CNTF) for amyotrophic lateral sclerosis/motor neuron disease. The Cochrane database of systematic reviews 2004(3):Cd004302.
18. Emerich DF, Thanos CG: Intracompartmental delivery of CNTF as therapy for Huntington's disease and retinitis pigmentosa. Current gene therapy 2006, 6(1):147-159.
19. Silani V, Braga M, Cardin V, Scarlato G: The pathogenesis of ALS: implications for treatment strategies. Neurol Neurochir Pol 2001, 35(1 Suppl):25-39.
20. Sarrouilhe D, di Tommaso A, Métayé T, Ladeveze V: Spinophilin: from partners to functions. Biochimie 2006, 88(9):1099-1113.
21. Wu L-J, Ren M, Wang H, Kim SS, Cao X, Zhuo M: Neurabin contributes to hippocampal long-term potentiation and contextual fear memory. PLoS ONE 2008, 3(1):e1407.
22. Beraki S, Diaz-Heijtz R, Tai F, Ogren SO: Effects of repeated treatment of phencyclidine on cognition and gene expression in C57BL/6 mice. The international journal of neuropsychopharmacology 2009, 12(2):243-255.
23. Stafstrom-Davis CA, Ouimet CC, Feng J, Allen PB, Greengard P, Houpt TA: Impaired conditioned taste aversion learning in spinophilin knockout mice. Learning & memory (Cold Spring Harbor, NY) 2001, 8(5):272-278.
24. Liauw J, Hoang S, Choi M, Eroglu C, Choi M, Sun G, Percy M, Wildmantobriner B, Bliss T, Guzman RG: Thrombospondins 1 and 2 are necessary for synaptic plasticity and functional recovery after stroke. Journal of Cerebral Blood Flow & Metabolism Official Journal of the International Society of Cerebral Blood Flow & Metabolism 2008, 28(10):1722-1732.
25. Brust TB, Cayabyab FS, Zhou N, Macvicar BA: p38 Mitogen-Activated Protein Kinase Contributes to Adenosine A1 Receptor-Mediated Synaptic Depression in Area CA1 of the Rat Hippocampus. Journal

of Neuroscience the Official Journal of the Society for Neuroscience 2006, 26(48):12427-12438.

26. Ono K, Han J: The p38 signal transduction pathway: activation and function. Cellular Signalling 2000, 12(1):1-13.
27. Huang Q, Liu X, Wu Y, Liao Y, Huang Y, Wei X, Ma M: P38 MAPK pathway mediates cognitive damage in pentylenetetrazole-induced epilepsy via apoptosis cascade. Epilepsy Res 2017, 133:89-92.
28. Chang K-W, Zong H-F, Ma K-G, Zhai W-Y, Yang W-N, Hu X-D, Xu J-H, Chen X-L, Ji S-F, Qian Y-H: Activation of α7 nicotinic acetylcholine receptor alleviates Aβ-induced neurotoxicity via downregulation of p38 and JNK MAPK signaling pathways. Neurochem Int 2018, 120:238-250.
29. Han Q, Lin Q, Huang P, Chen M, Hu X, Fu H, He S, Shen F, Zeng H, Deng Y: Microglia-derived IL-1β contributes to axon development disorders and synaptic deficit through p38-MAPK signal pathway in septic neonatal rats. J Neuroinflammation 2017, 14(1):52.
30. Habbas S, Santello M, Becker D, Stubbe H, Zappia G, Liaudet N, Klaus FR, Kollias G, Fontana A, Pryce CR et al: Neuroinflammatory TNFα Impairs Memory via Astrocyte Signaling. Cell 2015, 163(7):1730-1741.
31. Zhang Y, Fang X, Fan W, Tang W, Cai J, Song L, Zhang C: Interaction between BDNF and TNF-α genes in schizophrenia. Psychoneuroendocrinology 2018, 89:1-6.
32. Dhanda S, Gupta S, Halder A, Sunkaria A, Sandhir R: Systemic inflammation without gliosis mediates cognitive deficits through impaired BDNF expression in bile duct ligation model of hepatic encephalopathy. Brain Behav Immun 2018, 70:214-232.
33. Rizzo FR, Musella A, De Vito F, Fresegna D, Bullitta S, Vanni V, Guadalupi L, Stampanoni Bassi M, Buttari F, Mandolesi G et al: Tumor Necrosis Factor and Interleukin-1 Modulate Synaptic Plasticity during Neuroinflammation. Neural Plast 2018, 2018:8430123.
34. MacEwan DJCs: TNF receptor subtype signalling: differences and cellular consequences. 2002, 14(6):477-492.
35. Stellwagen D, Malenka RJN: Synaptic scaling mediated by glial TNF-alpha. 2006, 440(7087):1054-1059.
36. Beattie E, Stellwagen D, Morishita W, Bresnahan J, Ha B, Von Zastrow M, Beattie M, Malenka RJS: Control of synaptic strength by glial TNFalpha. 2002, 295(5563):2282-2285.
37. Cerpa W, Farías GG, Godoy JA, Fuenzalida M, Bonansco C, Inestrosa NC: Wnt-5a occludes Abeta oligomer-induced depression of glutamatergic transmission in hippocampal neurons. Molecular Neurodegeneration 2010, 5(1):3.
38. Chen J, Park CS, Tang SJ: Activity-dependent synaptic Wnt release regulates hippocampal long term potentiation. The Journal of biological chemistry 2006, 281(17):11910.
39. Varela-Moreiras G, Alonso-Aperte E, Rubio M, Gasso M, Deulofeu R, Alvarez L, Caballeria J, Rodes J, Mato J: Carbon tetrachloride-induced hepatic injury is associated with global dna hypomethylation and homocysteinemia: Effect of s-adenosylmethionine treatment . Hepatology 1995, 22(4):1310-1315.

40. Gogolla N, Galimberti I, Deguchi Y, Caroni P: Wnt signaling mediates experience-related regulation of synapse numbers and mossy fiber connectivities in the adult hippocampus. Neuron 2009, 62(4):510-525.
41. Oliva CA, Vargas JY, Inestrosa NC: Wnt signaling: role in LTP, neural networks and memory. Ageing Research Reviews 2013, 12(3):786.
42. Seib DR, Corsini NS, Ellwanger K, Plaas C, Mateos A, Pitzer C, Niehrs C, Celikel T, Martinvillalba A: Loss of Dickkopf-1 restores neurogenesis in old age and counteracts cognitive decline. Cell Stem Cell 2013, 12(2):204.
43. Tabatadze N, Tomas C, Mcgonigal R, Lin B, Schook A, Routtenberg A: Wnt transmembrane signaling and long-term spatial memory. Hippocampus 2012, 22(6):1228.
44. Kalani MY, Cheshier SH, Cord BJ, Bababeygy SR, Vogel H, Weissman IL, Palmer TD, Nusse R: Wnt-mediated self-renewal of neural stem/progenitor cells. Proceedings of the National Academy of Sciences of the United States of America 2008, 105(44):16970-16975.
45. Kuwabara T, Hsieh J, Muotri A, Yeo G, Warashina M, Lie DC, Moore L, Nakashima K, Asashima M, Gage FH: Wnt-mediated activation of NeuroD1 and retro-elements during adult neurogenesis. Nature Neuroscience 2009, 12(9):1097.
46. Toledo EM, Colombres M, Inestrosa NC: Wnt signaling in neuroprotection and stem cell differentiation. Progress in Neurobiology 2008, 86(3):281.
47. Ghanevati M, Miller CA: Phospho-β-catenin accumulation in alzheimer's disease and in aggresomes attributable to proteasome dysfunction. Journal of Molecular Neuroscience 2005, 25(1):79-94.
48. Zhang Z, Hartmann H, Do VM, Abramowski D, Sturchlerpierrat C, Staufenbiel M, Sommer B, Van dWM, Clevers H, Saftig P: Destabilization of beta-catenin by mutations in presenilin-1 potentiates neuronal apoptosis. Nature 1998, 395(6703):698-702.
49. Ding S, Xu Z, Yang J, Liu L, Huang X, Wang X, Zhuge Q: The Involvement of the Decrease of Astrocytic Wnt5a in the Cognitive Decline in Minimal Hepatic Encephalopathy. Molecular neurobiology 2016.
50. Budnik V, Salinas PC: Wnt signaling during synaptic development and plasticity. Current Opinion in Neurobiology 2011, 21(1):151.
51. Hall AC, Lucas FR, Salinas PC: Axonal Remodeling and Synaptic Differentiation in the Cerebellum Is Regulated by WNT-7a Signaling. Cell 2000, 100(5):525-535.
52. Ahmad-Annuar A, Ciani L, Simeonidis I, Herreros J, Fredj NB, Rosso SB, Hall A, Brickley S, Salinas PC: Ahmad-Annuar, A. et al. Signaling across the synapse: a role for Wnt and Dishevelled in presynaptic assembly and neurotransmitter release. J. Cell Biol. 174, 127-139. Journal of Cell Biology 2006, 174(1):127-139.
53. Garcia P, Youssef I, Utvik JK, Florent-Béchard S, Barthélémy V, Malaplate-Armand C, Kriem B, Stenger C, Koziel V, Olivier J-L et al: Ciliary neurotrophic factor cell-based delivery prevents synaptic impairment and improves memory in mouse models of Alzheimer's disease. J Neurosci 2010, 30(22):7516-7527.

54. Nai Q, Wang X, Jin Y, Sun D, Li M, Hu B, Zhang X: Ciliary neurotrophic factor enhances nicotinic synaptic transmission in sympathetic neurons. J Neurosci Res 2010, 88(4):887-895.
55. Tsukada M, Prokscha A, Oldekamp J, Eichele G: Identification of neurabin II as a novel doublecortin interacting protein. Mechanisms of development 2003, 120(9):1033-1043.
56. Muly EC, Smith Y, Allen P, Greengard P: Subcellular distribution of spinophilin immunolabeling in primate prefrontal cortex: localization to and within dendritic spines. J Comp Neurol 2004, 469(2):185-197.
57. Ouimet CC, Katona I, Allen P, Freund TF, Greengard P: Cellular and subcellular distribution of spinophilin, a PP1 regulatory protein that bundles F-actin in dendritic spines. J Comp Neurol 2004, 479(4):374-388.
58. Satoh A, Nakanishi H, Obaishi H, Wada M, Takahashi K, Satoh K, Hirao K, Nishioka H, Hata Y, Mizoguchi A et al: Neurabin-II/spinophilin. An actin filament-binding protein with one pdz domain localized at cadherin-based cell-cell adhesion sites. J Biol Chem 1998, 273(6):3470-3475.
59. Satoh A, Nakanishi H, Obaishi H, Wada M, Takahashi K, Satoh K, Hirao K, Nishioka H, Hata Y, Mizoguchi A et al: Neurabin-II/spinophilin. An actin filament-binding protein with one pdz domain localized at cadherin-based cell-cell adhesion sites. J Biol Chem 1998, 273(6):3470-3475.
60. Yan Z, Hsieh-Wilson L, Feng J, Tomizawa K, Allen PB, Fienberg AA, Nairn AC, Greengard P: Protein phosphatase 1 modulation of neostriatal AMPA channels: regulation by DARPP-32 and spinophilin. Nat Neurosci 1999, 2(1):13-17.
61. Akram A, Christoffel D, Rocher AB, Bouras C, Kövari E, Perl DP, Morrison JH, Herrmann FR, Haroutunian V, Giannakopoulos P et al: Stereologic estimates of total spinophilin-immunoreactive spine number in area 9 and the CA1 field: relationship with the progression of Alzheimer's disease. Neurobiol Aging 2008, 29(9):1296-1307.

Figures

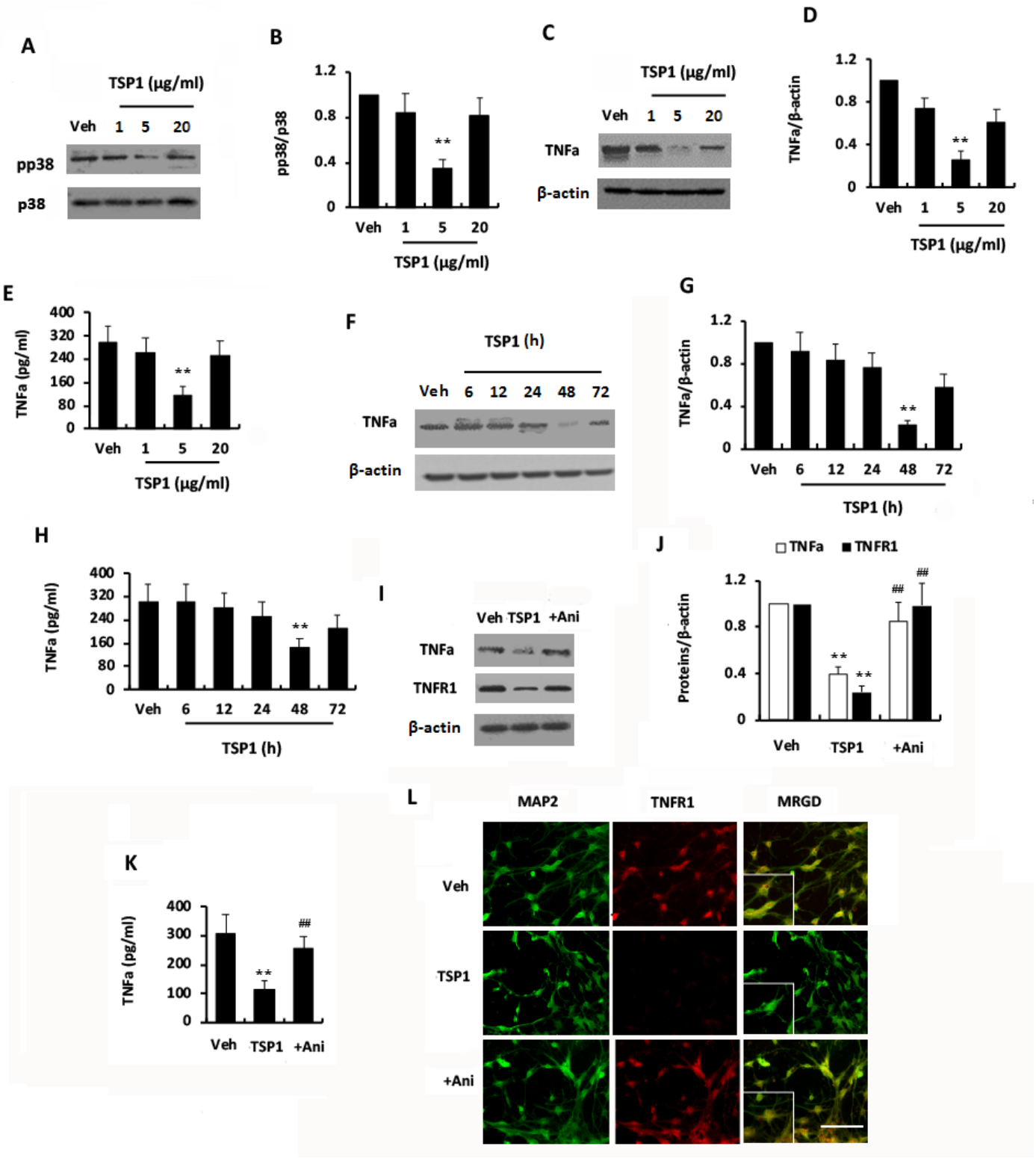

Figure 1

TSP-1 inactivated p38MAPK/TNFα signaling in vitro (A–D) Immunoblotting analysis and subsequent densitometry of lysate from PC12 cells stimulated with various concentrations of TSP1 using antibodies against pp38 /p38 (A, B) or TNFα/β-actin (C, D). (E) ELISA for TNFα content of supernatants from PC12 cells stimulated with various concentrations of TSP1. (F, G) Immunoblotting analysis and subsequent densitometry of lysate from PC12 cells stimulated with FGF2 for various time points using anti-TNFα and

anti-β-actin antibodies. (H) ELISA for TNFα level of supernatants from PC12 cells stimulated with TSP1 for various time points. (I,J) Immunoblotting analysis and subsequent densitometry of lysate from PHNs treated with TSP1 in the presence of anisomycin using antibodies against TNFα/TNFR1/β-actin. (K) ELISA to evaluate the TNFα content of supernatants from PHNs treated with TSP1 in the presence of anisomycin. (L) Immunostaining of PHNs treated with TSP1 in the presence of anisomycin using antibodies against TNFR1 (red) and MAP2 (green). Data are shown as mean ± SD. *P < 0.05, **P < 0.01 vs. vehicle/Flag/Scr siRNA-treated group; #P < 0.05, ##P < 0.01 vs. Flag-TSP1/TSP1 siRNA-treated group. Scr, scrambled. Scale bar, 25 μm. MRGD, merged image. TSP1, thrombospondin; SB, SB202190; Ani, anisomycin; Len, lenalidomide.

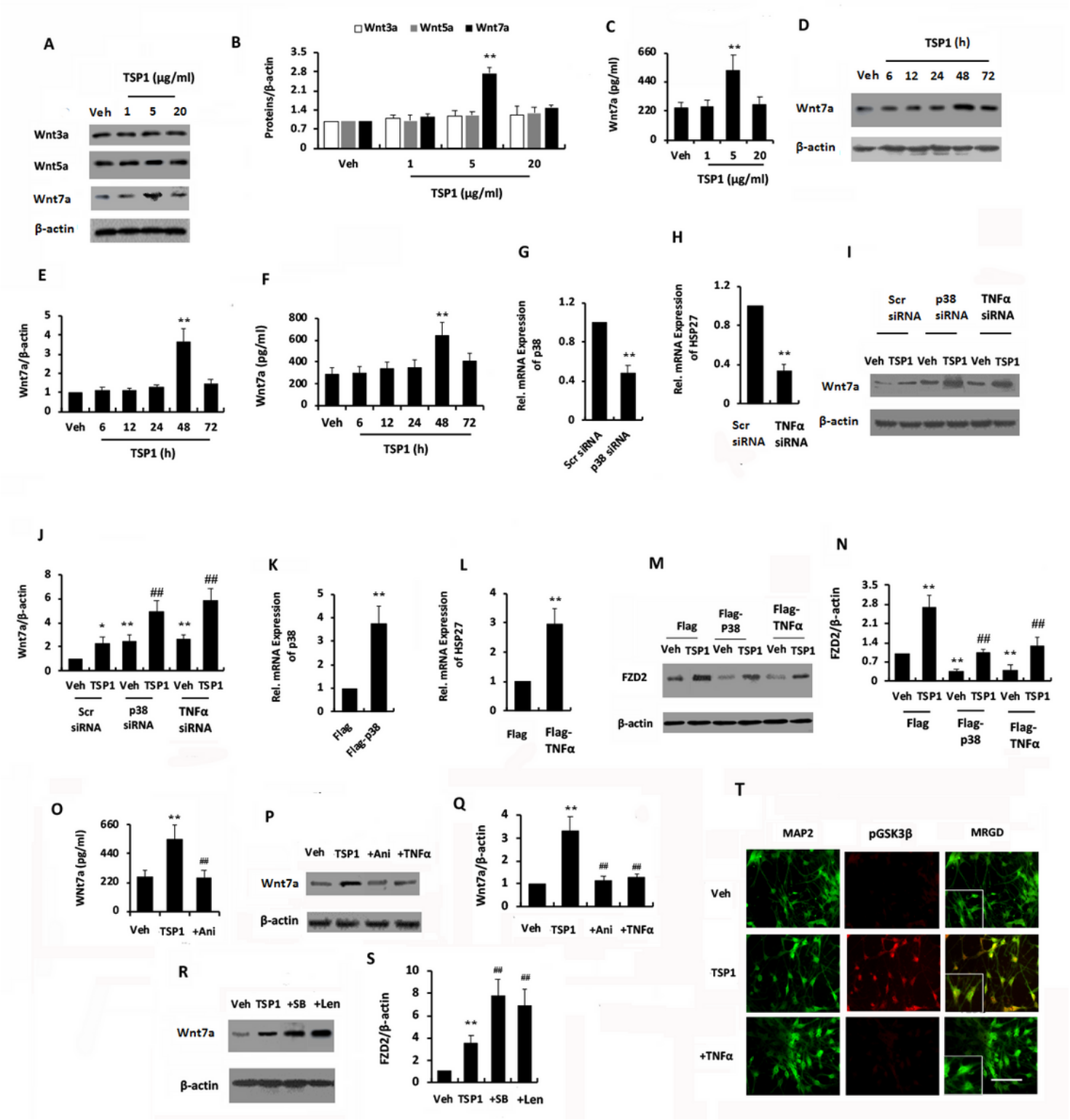

Figure 2

TSP1 activated Wnt7a signaling via p38/TNFα signaling. (A, B) Immunoblotting analysis of the lysate from PC12 cells stimulated with various concentrations of TSP1 using antibodies against Wnt3a/Wnt5a/Wnt7a/β-actin and subsequent densitometry. (C) ELISA for Wnt7a content of supernatants from PC12 cells stimulated with various concentrations of TSP1. (D, E) Immunoblotting analysis of lysate from PC12 cells stimulated with TSP1 for various time points, using antibodies against Wnt7a/β-actin

and subsequent densitometry. (F) ELISA for Wnt7a level of supernatants from PC12 cells stimulated with TSP1 for various time points. (G, H) qPCR analysis of p38/TNFα mRNA of PC12 cells transfected with p38/TNFα siRNA plasmid. (I, J) Immunoblotting analysis of PC12 cells transfected with p38/TNFα siRNA plasmid in the presence of TSP1 using antibodies against Wnt7a and subsequent densitometry. (K, L) qPCR analysis of p38/TNFα mRNA of PC12 cells transfected with p38/TNFα overexpression plasmid. (M, N) Immunoblotting analysis of PC12 cells transfected with p38/TNFα overexpression plasmid in the presence of TSP1 using antibodies against FZD2 and subsequent densitometry. (O) ELISA for Wnt7a content of supernatants from PHNs treated with TSP1 in the presence of anisomycin. (P-S) Immunoblotting analysis of PHNs treated with TSP1 in the presence of anisomycin, TNFα (P, Q), SB202190 or lenalidomide (R, S) using antibodies against Wnt7a and subsequent densitometry. (T) Immunostaining of PHNs treated with TSP1 in the presence of TNFα against pGSK3β (red) and MAP2 (green). Data are shown as mean ± SD. *P < 0.05, **P < 0.01 vs. vehicle/Flag/Scr siRNA/vehicle+scr siRNA/vehicle+Flag-treated group; #P < 0.05, ##P < 0.01 vs. Flag-TSP1/TSP1 siRNA/TSP1+scr siRNA/TSP1+Flag-treated group. Scr, scrambled. Scale bar, 25 μm. MRGD, merged image.

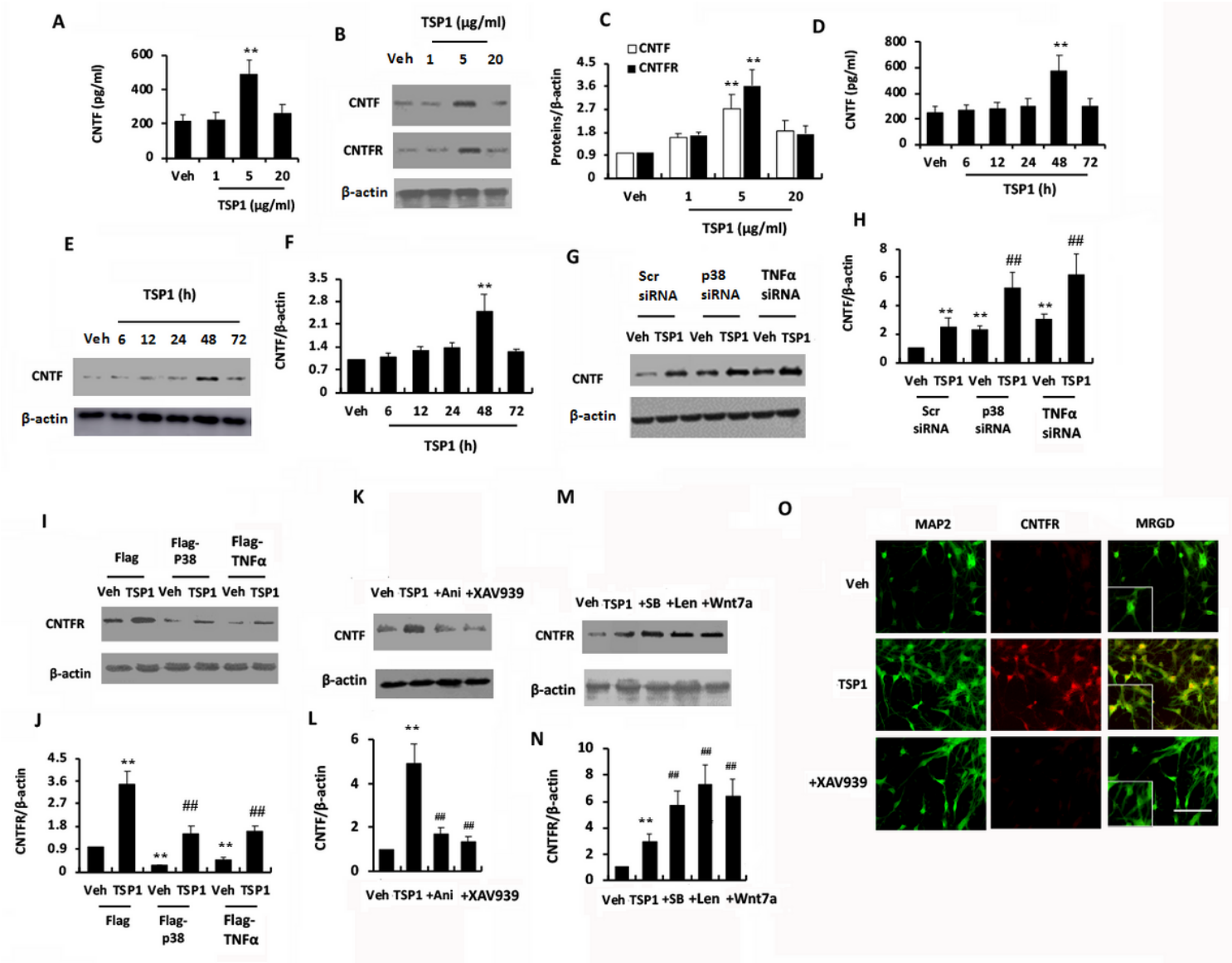

Figure 3

TSP1 activated CNTF signaling via p38/TNFα. (A, B) Immunoblotting analysis of lysate from PC12 cells stimulated with various concentrations of TSP1 using antibodies against CNTF/β-actin and subsequent densitometry. (C) ELISA to assess the CNTF content in the supernatants from PC12 cells stimulated with various concentrations of TSP1. (D, E) Immunoblotting analysis of lysate from PC12 cells stimulated with TSP1 for various time points using antibodies against CNTF/β-actin and subsequent densitometry. (F) ELISA for CNTF level of supernatants from PC12 cells stimulated with TSP1 for various time points. (G, H) Immunoblotting analysis of PC12 cells transfected with p38/TNFα siRNA plasmid in the presence of TSP1 using antibodies against CNTF and subsequent densitometry. (I, J) Immunoblotting analysis of PC12 cells transfected with p38/TNFα overexpression plasmid in the presence of TSP1 using antibodies against CNTFR and subsequent densitometry. (K, L) Immunoblotting analysis of PHNs treated with TSP1 in the presence of anisomycin or XAV939 using antibodies against CNTF and subsequent densitometry. (M, N) Immunoblotting analysis of PHNs treated with TSP1 in the presence of SB202190, lenalidomide, or Wnt7a using antibodies against CNTFR and subsequent densitometry. (O) Immunostaining of PHNs treated with TSP1 in the presence of XAV939 against CNTFR (red) and MAP2 (green). Scale bar, 2 μm. Data are shown as mean ± SD. *P < 0.05, **P < 0.01 vs. vehicle/Flag/Scr siRNA/vehicle+scr siRNA/vehicle+Flag-treated group; #P < 0.05, ##P < 0.01 vs. Flag-TSP1/TSP1 siRNA/TSP1+scr siRNA/TSP1+Flag-treated group. Scr, scrambled. Scale bar, 25 μm. MRGD, merged image.

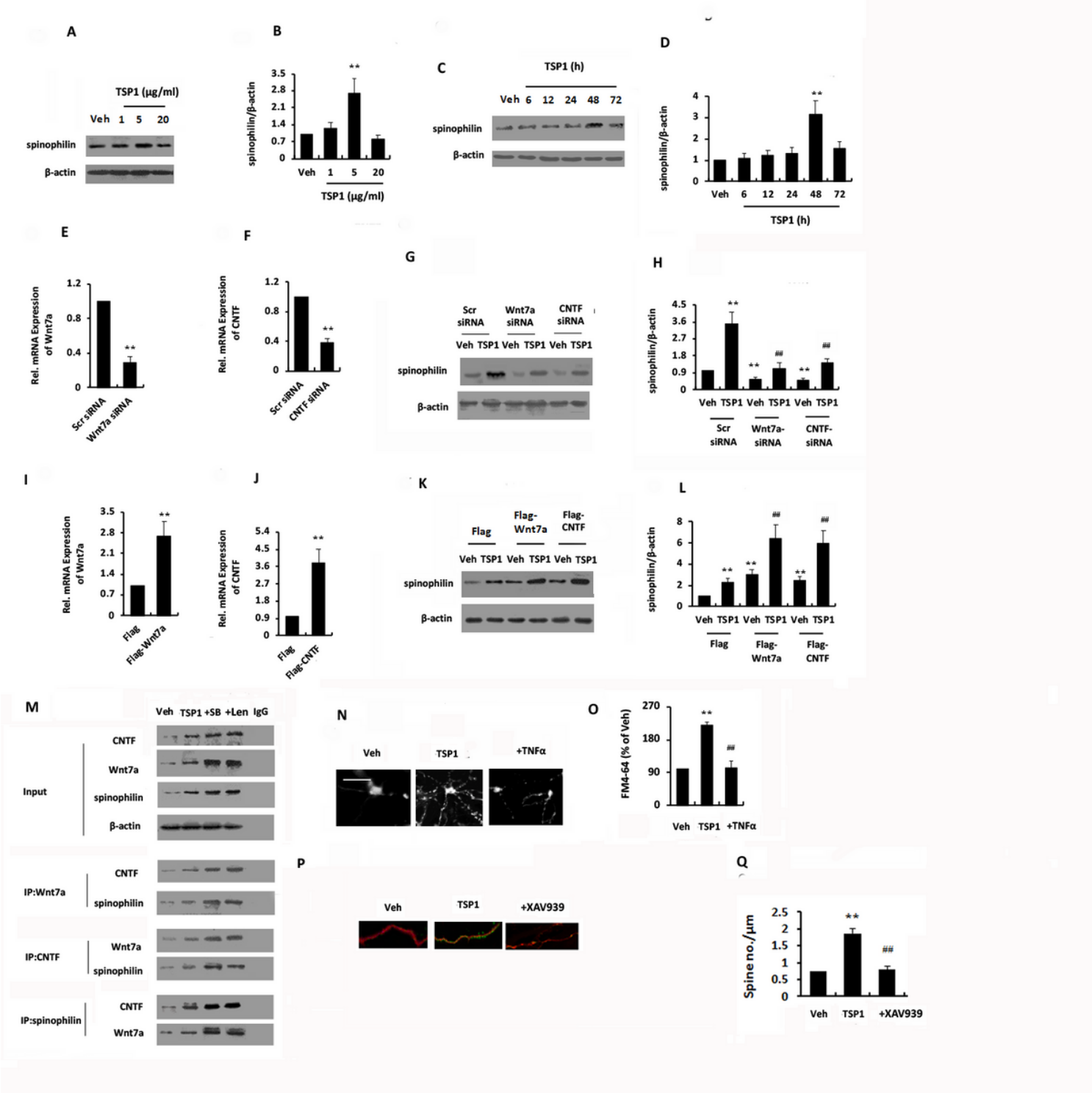

Figure 4

TSP1 increased spinophilin expression via Wnt7a/CNTF signaling in vitro. (A, B) Immunoblotting analysis of PC12 cells stimulated with various concentrations of TSP1 using anti-spinophilin and anti-β-actin antibodies and subsequent densitometry. (C, D) Immunoblotting analysis of PC12 cells treated with TSP1 for various time points using antibodies against spinophilin and β-actin and subsequent densitometry. (E, F) qPCR analysis of Wnt7a/CNTF mRNA in PC12 cells transfected with Wnt7a/CNTF siRNA plasmid. (G, H) Immunoblotting analysis of PC12 cells transfected with Wnt7a/CNTF siRNA plasmid in the presence

of TSP1 using antibodies against spinophilin and subsequent densitometry. (I, J) qPCR analysis of Wnt7a/CNTF mRNA in PC12 cells transfected with Wnt7a/CNTF overexpression plasmid. (K, L) Immunoblotting analysis of PC12 cells transfected with Wnt7a/CNTF overexpression plasmid in the presence of TSP1 using antibodies against spinophilin and subsequent densitometry. (M) Coimmunoprecipitation analysis of hippocampal lysates of PHNs treated with TSP1 in the presence of SB202190 or lenalidomide for the association among Wnt7a, CNTF, and spinophilin. (N, O) Representative image of FM4-64 staining of functional presynaptic terminals in PHNs treated with TSP1 in the presence of TNFα. (O) shows the quantitative analysis of changes as an average in FM4-64 puncta intensity. (P, Q) Immunostaining of PHNs treated with TSP1 in the presence of XAV939 using antibodies against MAP2 (red) and vGluT1 (green). Red signals indicate MAP2 for microtubule staining and green signals indicate vGluT1 for detecting excitatory synapses. Synaptic density (Q) was analyzed by evaluating green signals (vGluT1-positive dendritic spines) using ImageJ, and expressed per 1 μm of apical dendrite. Data are shown as mean ± SD. *P < 0.05, **P < 0.01 vs. vehicle/Flag/Scr siRNA/vehicle+scr siRNA/vehicle+Flag-treated group; #P < 0.05, ##P < 0.01 vs. Flag-TSP1/TSP1 siRNA/TSP1+scr siRNA/TSP1+Flag-treated group. Scr, scrambled. Scale bar, 25 μm. MRGD, merged image.

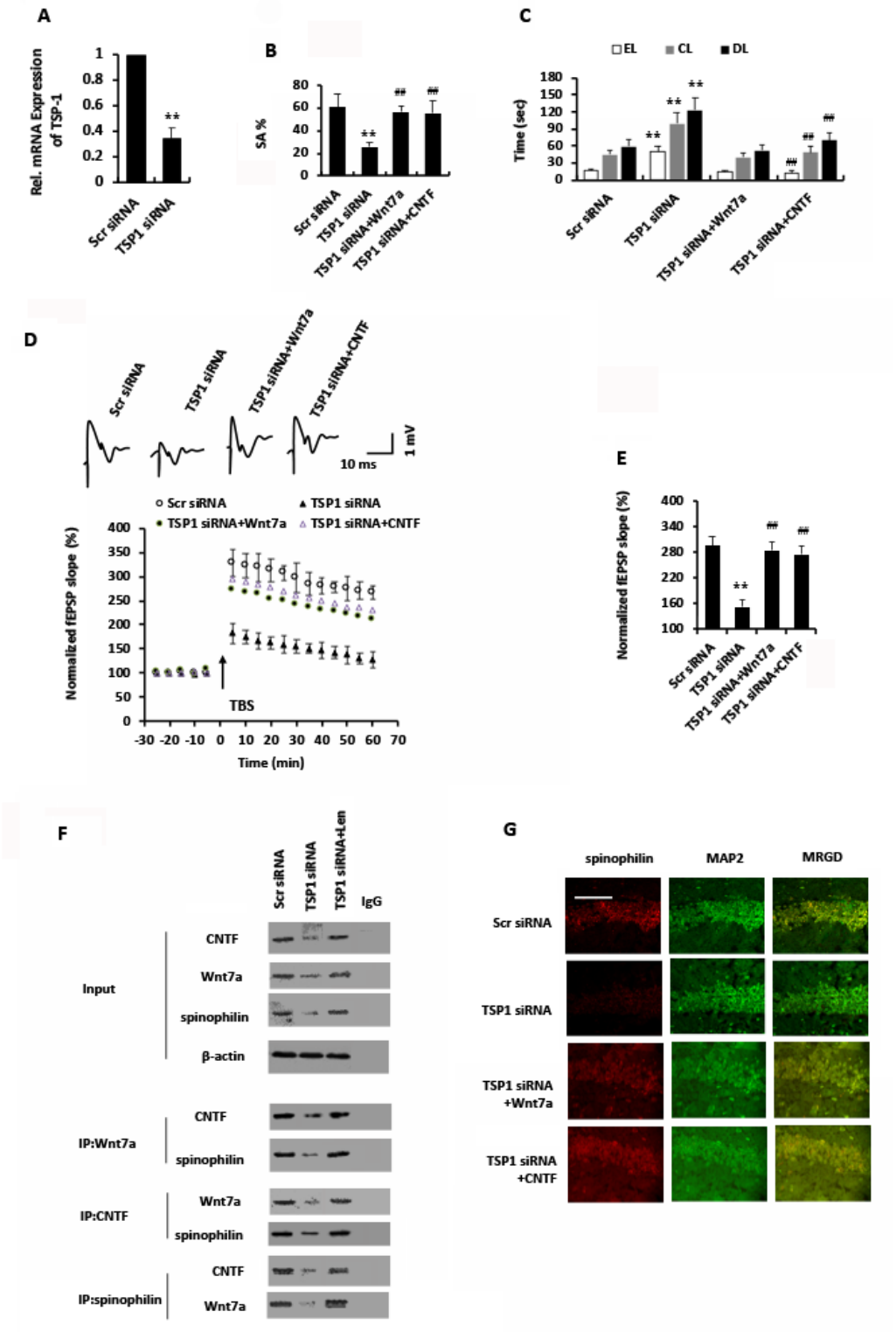

Figure 5

The interaction of Wnt7a/CNTF with spinophilin was impaired in TSP1 knockdown mice. (A) qPCR analysis of TSP1 mRNA of lysates from the hippocampus of WT mice injected with TSP1 siRNA plasmid. (B) The spontaneously altered percentage (SA%) in the YM of mice hippocampally injected with TSP1 siRNA plasmid together with Wnt7a or CNTF. (C) The data of WFT (EL, entry latency; CL, contacting latency; DL, drinking latency) of mice hippocampally injected with TSP1 siRNA plasmid together with

Wnt7a or CNTF. (D) Input/output (I/O) curves relating the slope of fEPSP to the amplitude of presynaptic fiber volley at various stimuli intensities in the CA1 region of WT mice hippocampally injected with TSP1 siRNA plasmid together with Wnt7a or CNTF. (E) The average slope of I/O curves of WT mice hippocampally injected with TSP1 siRNA plasmid together with Wnt7a or CNTF.(F) Coimmunoprecipitation analysis of hippocampal lysates of WT mice hippocampally injected with TSP1 siRNA plasmid together with lenalidomide for the association among Wnt7a, CNTF and spinophilin. (G) Immunostaining of free-floating hippocampal sections from WT mice hippocampally injected with TSP1 siRNA plasmid together with Wnt7a or CNTF using antibodies against spinophilin (red) and MAP2 (green). Data are shown as mean ± SD. *P < 0.05, **P < 0.01 vs. Scr siRNA-knockdown mice; #P < 0.05, ##P < 0.01 vs. TSP1 siRNA-knockdown mice. Scr, scrambled. Scale bar, 25 μm. MRGD, merged image.

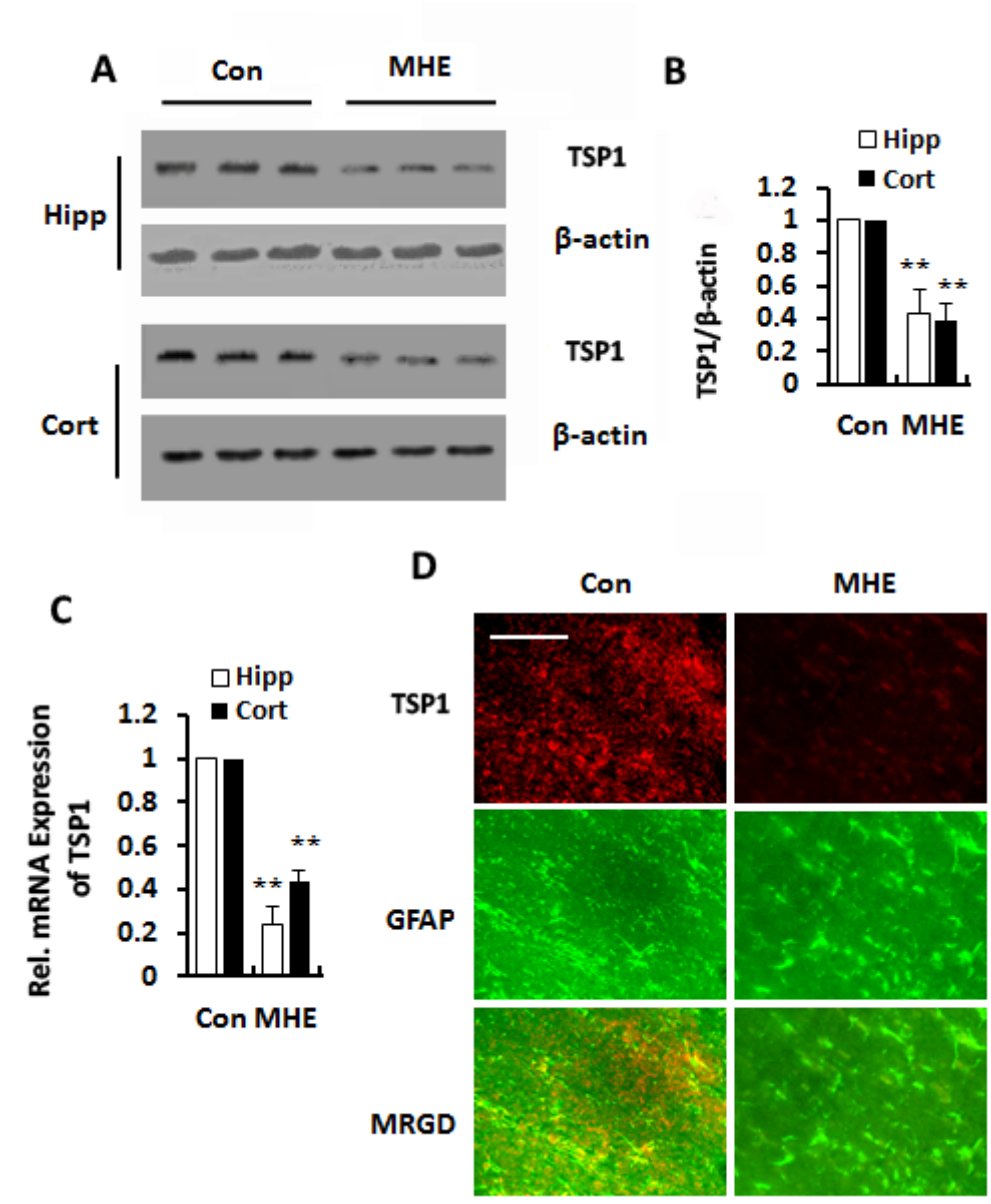

Figure 6

TSP1 expression was decreased in MHE rats. (A, B) Immunoblotting analysis of hippocampal or cortical homogenates from MHE rats using antibodies against TSP1 and β-actin, followed by densitometry

analysis. (C) qPCR analysis of TSP1 mRNA in lysates from hippocampus or cerebral cortices of MHE rats. (D) Immunostaining of free-floating cortical sections from MHE rats using antibodies against TSP1 (red) and MAP2 (green).Data are shown as mean ± SD. *P < 0.05, **P < 0.01 vs. control rats. Scale bar, 25 μm. MRGD, merged image.

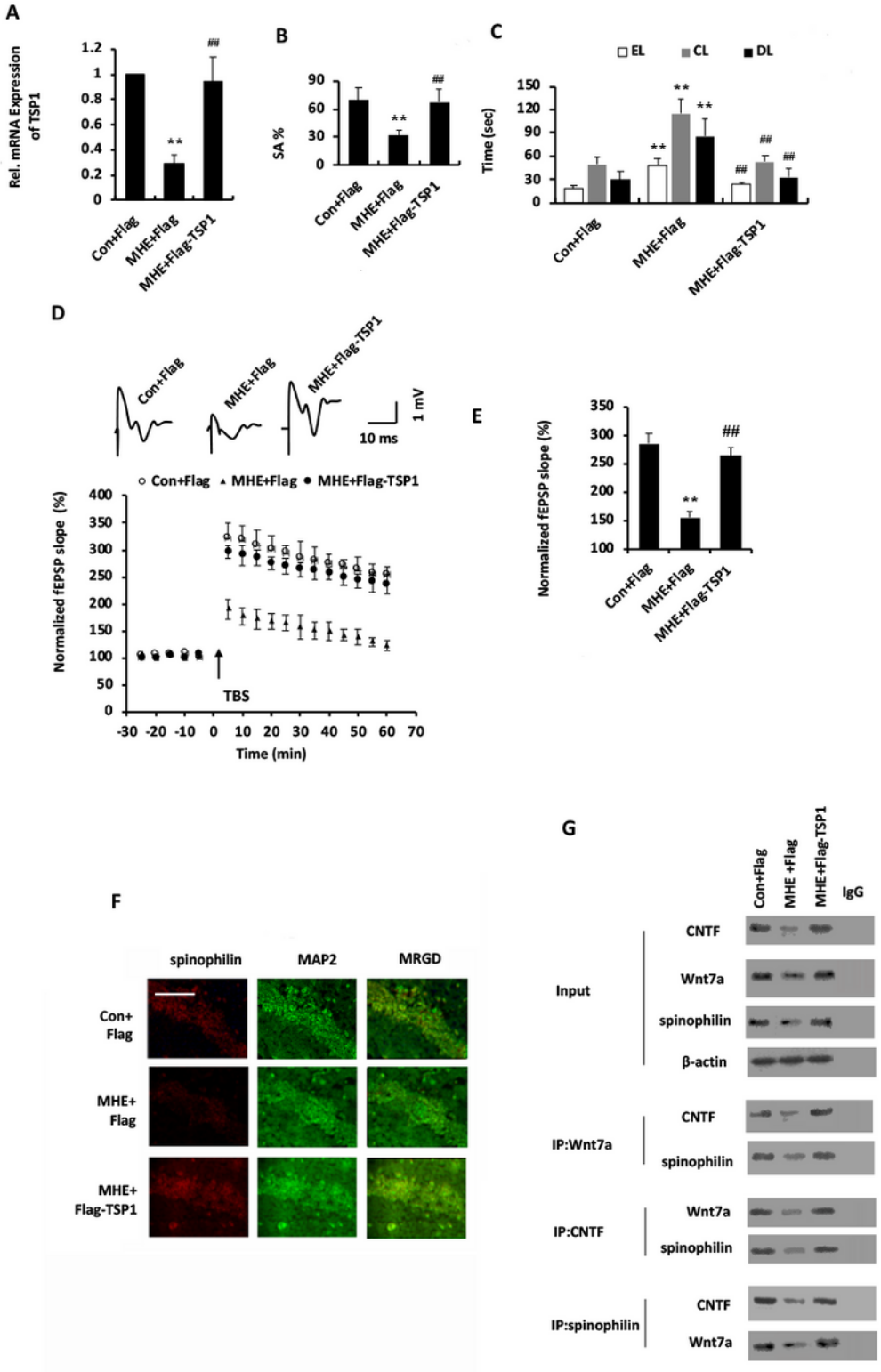

Figure 7

TSP1 overexpression ameliorated the cognitive decline and the impairment of Wnt7a/CNTF and spinophilin interaction in MHE rats. (A) qPCR analysis of TSP1 mRNA extracted from the lysates of hippocampus of MHE rats injected with TSP1 overexpression plasmid. (B) Spontaneous alternation percentage (SA%) in YM of MHE rats hippocampally injected with TSP1 overexpression plasmid. (C) Results of WFT (EL, entry latency; CL, contacting latency; DL, drinking latency) of MHE rats hippocampally injected with TSP1 overexpression plasmid. (D) Input/output (I/O) curves relating the slope of fEPSP to the amplitude of presynaptic fiber volley at various stimulus intensities in the CA1 region of MHE rats hippocampally injected with TSP1 overexpression plasmid. (E) The average slope of I/O curves of MHE rats hippocampally injected with TSP1 overexpression plasmid. (F) Immunostaining of free-floating hippocampal sections from MHE rats hippocampally injected with TSP1 overexpression plasmid using antibodies against spinophilin (red) and MAP2 (green). (G) Coimmunoprecipitation analysis of hippocampal lysates of MHE rats hippocampally injected with TSP1 overexpression plasmid to assess the association among Wnt7a, CNTF, and spinophilin. Data are represented as mean ± SD. *P < 0.05, **P < 0.01 vs. control+Flag rats; #P < 0.05, ##P < 0.01 vs. MHE+Flag rats. Scale bar, 25 μm. MRGD, merged image.